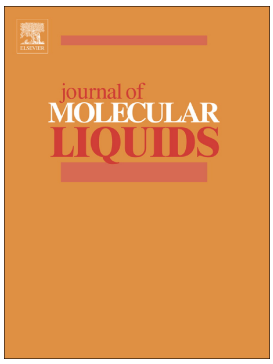

Computational optimization of bioadsorbents for the removal of pharmaceuticals from water

José M. Pereira, Vânia Calisto, Sérgio M. Santos

PII: S0167-7322(18)35713-1
DOI: https://doi.org/10.1016/j.molliq.2019.01.167
Reference: MOLLIQ 10398

To appear in: *Journal of Molecular Liquids*

Received date: 4 November 2018
Revised date: 29 January 2019
Accepted date: 31 January 2019

Please cite this article as: J.M. Pereira, V. Calisto and S.M. Santos, Computational optimization of bioadsorbents for the removal of pharmaceuticals from water, Journal of Molecular Liquids, https://doi.org/10.1016/j.molliq.2019.01.167

Computational optimization of bioadsorbents for the removal of pharmaceuticals from water

José M. Pereira[a], Vânia Calisto[b], Sérgio M. Santos[c]*

[a] Department of Chemistry, University of Aveiro, 3810-193 Aveiro, Portugal

[b] Department of Chemistry and CESAM (Centre for Environmental and Marine Studies), University of Aveiro, 3810-193 Aveiro, Portugal

[c] Department of Chemistry and CICECO (Aveiro Institute of Materials), University of Aveiro, 3810-193 Aveiro, Portugal

* corresponding author: sergio.santos@ua.pt

ABSTRACT

Pharmaceutically active ingredients are amongst the most persistent wastewater contaminants, resisting to wastewater treatment plants (WWTP) conventional processes, and some of them are proved to pose serious threats to organisms and the environment. In this context, adsorption by activated carbons (AC) is one of the most promising methodologies for the removal of pharmaceuticals from water due to its versatility and high removal efficiency. However, ACs are expensive and therefore not widely applied in WWTP. Primary sludge from paper mills has been previously appointed as a potential inexpensive and renewable source of carbon for AC production by pyrolysis. Computational chemistry may help shed some light into the molecular mechanisms underlying the adsorption of organic pollutants onto ACs. In this context, CarbGen, an online tool for Virtual Porous Carbon (VPC) models creation, was developed and made available for public use. A quantitatively validated model based on both physical and chemical characteristics of an experimentally produced AC is proposed. The produced model is in agreement with obtained experimental data in terms of elemental composition, functional group content and surface area. Grand Canonical Monte Carlo (GCMC) studies were performed on various VPC models with different levels of oxygen content, revealing the importance of electrostatic mechanisms in adsorption, with different degrees depending on the pharmaceutical molecular characteristics. The results further reinforce the importance of functional groups in future VPC models for correct molecular modelling.

Keywords: ADSORPTION; WATER TREATMENT; MOLECULAR DYNAMICS; MOLECULAR MODELLING; MONTE-CARLO SIMULATIONS; VIRTUAL POROUS CARBONS

1. INTRODUCTION

Both humans and animals have greatly benefited from the last century advances in medicine. However, due to several factors, such as the discovery of new drugs, increase in population and industrialization levels, demographic ageing and expiration of patents, an increase in drug production, consumption and disregarded disposal has been verified (1–3). The current situation poses severe threats to human health and non-target organisms and is a serious cause of environmental damage (4–7). Therefore, some pharmaceutical compounds are now regarded as priority substances in the field of water policy according to European directives (8).

Wastewater treatment plants (WWTPs) receive contaminated effluents from drug manufacturing plants and municipal sewage systems (9). It has been reported that about 64% of these emerging contaminants are only partially removed (< 50%) while up to 9% are not removed at all by the standard treatment processes in WWTPs (10). Therefore, alternative processes for the removal of pharmaceuticals from water have been previously proposed (11–14).

In this context, adsorption of contaminants by activated carbons (AC) emerges as an optimistic solution, with advantages such as versatile usage, high removal efficiencies and the ability to regenerate and reuse spent adsorbents (15), even though it is still not widely used because of its high-cost (16) and the fact that it does not mineralize the contaminants (17). Traditionally, ACs are produced from fossil feedstocks such as bituminous coal and oil. Multiple renewable feedstocks have been previously appointed as potential precursors for the production of AC, such as coconut shell (18), eucalyptus wood (19) or sugar cane bagasse (20), among others (21,22). Such pursuit has the aim of lowering the production costs, increasing feedstock availability and reducing particulate matter generation or heavy metal contamination during carbonization processes (23,24).

More recently, paper industry primary sludge (PS)-based ACs were also produced and evaluated for the removal of pharmaceuticals from water, showing promising results (25–32).

Over 30 million tons of this waste are produced every year around the globe (33), with its disposal being currently a major issue. Traditionally, it involves landfilling or energy production through incineration/combustion. However, such solutions are rapidly becoming unsustainable based on a number of factors, such as economic disadvantages, leachate production, landfill space depletion and atmospheric contamination concerns (34–36). Therefore, harnessing of this material for AC production is an innovative handling strategy.

Optimization of ACs has been an open area of research. Some authors point functional group interactions as the main force guiding molecular adsorption, while others assign it to microporous structure and specific surface areas (37). Therefore, deeper insights into the interactions between adsorbates and the AC are necessary. This would allow the modulation of the AC characteristics in order to increase adsorption capacities and rates or target compound selectivity.

Molecular modelling of ACs allows for detailed analysis of the interactions between the adsorbent and the target molecules. Virtual Porous Carbon (VPC) models have been previously developed and explored to provide insights regarding the adsorption mechanism. In the most recent studies, VPC models incorporated complex microcrystallites with some surface functional groups (38–41). However, reconstruction methods have commonly relied on multiple literature sources of experimental data as the basis for the model parametrization, and have mostly focused on physical characteristics of the carbon materials, such as pore distribution, often ignoring the importance of surface chemistry on the model (42). The possibility to adapt computational models in a quantitative manner to a real sample of AC naturally emerges as an interesting development in the field of AC modelling and as a tool for designing improvements in AC production.

Hence, the present work objectives are to produce experimental AC samples from an alternative carbon source (PS), fully characterize their structural and chemical nature and use the obtained data to parametrize and develop a quantitative computational model of AC in a simple and reproducible way. With this aim in mind, CarbGen (carbgen.web.ua.pt), a new

computational tool, was developed and made available to the scientific community in an effort to expedite quantitative modelling of ACs. Furthermore, the developed VPC models can be applied in the exploration of the effect of carbon surface chemistry in the adsorption capacity of pharmaceuticals in aqueous systems. The underlying mechanisms behind CarbGen can be further explored in the Supporting Information.

2. METHODS AND MATERIALS

AC samples were prepared using paper mill PS as precursor. The sludge was obtained from a Portuguese factory operating an elemental chlorine free kraft process, using *Eucalyptus globulus*. The AC samples were subjected to 6 characterization techniques: Point of Zero Charge (PZC) determination, proximate and ultimate analysis, specific surface area determination (S_{BET}), X-Ray Photoelectron Spectroscopy (XPS) and Scanning/Transmission Electron Microscopy (SEM/TEM).

The gathered data was then used in the formulation and validation of a new VPC model for AC. A clustering process was devised and employed using molecular dynamics approaches, and pharmaceutical adsorption was quantified using Grand Canonical Monte Carlo (GCMC) techniques, as detailed in the next sections.

2.1) AC sample preparation

AC production from PS have been previously optimized (32). PS was dried at 60 ºC in an oven, for 24h, and grinded with a blade mill before further treatment. ACs were produced by chemical activation with potassium carbonate (K_2CO_3), in a proportion of 1:1 (*w/w*). The activating agent solution was prepared with the proportion of 50 mL of distilled water (H_2O_d) to 15 g of K_2CO_3. PS was impregnated during 1 h in an ultrasonic bath and the impregnated PS was left to dry at room temperature. Pyrolysis of the impregnated PS was performed in porcelain crucibles in a furnace muffle under inert atmosphere with a nitrogen flow, at 800ºC, heating rate of 10 ºC min^{-1} and residence time of 150 minutes. Nitrogen flow was maintained

during the cooling of the furnace. A washing step using HCl in a proportion of 1.2 g of AC to 40 mL of 1.2 M HCl (37%, Panreac) was employed. The carbon material and the washing solution were kept in contact for 1 h. The resulting slurry was vacuum filtered and washed with distilled water until neutral pH of the washing leachate was achieved. The samples were then dried for 7 h in an oven at 105 ºC, and subsequently grinded with a blade mill.

2.2) Material characterization

2.2.1) PZC

PZC was determined by batch equilibration. 2 mg of the AC sample were shaken in polypropylene tubes with 10 mL of NaCl 0.1 M (≥99.5%, Fluka) solution, for 12 h in a overhead shaker at 25 ºC, at different pH values (from 2 to 12). Initial pH values were measured and adjusted using 0.1 M and 0.05 M HCl (37%, Panreac), and 0.1 M and 0.05 M NaOH (99.3%, José Manuel Gomes dos Santos, Portugal). The final pH was measured and the PZC was determined by plotting the ΔpH ($pH_f - pH_i$) versus the pH_i. The PZC is the pH value at which the curve intersects the x-axis.

2.2.2) Proximate and ultimate analysis

Standard methods to determine the moisture (*UNE 32002*), volatile matter (*UNE 32019*) and ash content (*UNE 32004*) were employed in a LECO TGA-601 automatic analyzer, for proximate analysis. The remaining fraction after ash and volatile matter (at dry basis) was determined to be the fixed carbon content.

Ultimate analysis was performed in a LECO CHNS-932 analyzer, determining the content in carbon (*C*), hydrogen (*H*), nitrogen (*N*) and sulfur (*S*) in the samples. Oxygen (*O*) content was determined by difference at dry and ash free basis.

2.2.3) S_{BET}

S_{BET} was determined on a Micromeritics ASAP2420 apparatus using the N_2 adsorption isotherm at -196ºC and Brunauer–Emmett–Teller equation in the relative pressure range 0.01–0.1. Degasification process of the sample was carried overnight. Additionally, average pore

width and total pore volume were also determined from the amount of nitrogen adsorbed at a relative pressure of 0.99.

2.2.4) XPS

Functional group content was determined by XPS analysis. Spectra were acquired in an Ultra High Vacuum system with a base pressure of $2x10^{-10}$ mbar. The system is equipped with a hemispherical electron energy analyzer (SPECS Phoibos 150), a delay-line detector and a monochromatic AlKα (1486.74 eV) X-ray source. High resolution spectra were recorded at normal emission take-off angle and with a pass-energy of 20 eV, which provides an overall instrumental peak broadening of 0.5 eV.

2.2.5) SEM/TEM

SEM images were obtained at the following magnifications: 300x, 1 000x, 3 000x, 10 000x, 30 000x and 50 000x, using a Hitachi SU-70. The apparatus was also used to perform EDS analysis using a Bruker QUANTAX 400.

TEM images were obtained using a HR-(EF)TEM JEOL 2200FS microscope at the following magnifications: 5 000x, 20 000x, 50 000x, 80 000x, 100 000x, 150 000x and 200 000x.

2.3) VPC Clustering

Atom types for all molecules used in the present work were extracted from the Generalized Amber Force Field (GAFF)(43) and simplified for this model application. For this matter, non-bonded interactions were considered to be Lennard-Jones pairs, with Lorentz-Berthelot combination rules as defined in GAFF. Lennard-Jones and electrostatics 1-4 interactions were multiplied by 0.5 and 0.833, respectively.

AC model parametrization and development is further explored in section 3. All molecule optimizations were carried by Density Functional Theory (DFT) at the B3LYP/6-31G* level using Gaussian09 (44). Charge determination on the optimized structures was performed at the HF/6-31G* level, from which Restrained Electrostatic Potential (RESP) partial charges were obtained using Antechamber (45).

Molecular dynamics simulations for VPC clustering processes were performed using the GROMACS software (46), in 125 nm^3 cubic boxes (5 nm each side) with periodic boundary conditions (PBC) applied. All simulation stages used the Verlet cut-off scheme for neighbor searching, particle-mesh Ewald for electrostatics beyond 12 Å cut-off and 12 Å cut-off for *van der* Waals interactions. Water molecules were modeled according to the TIP3P model (47). The clustering process is further explained in section 3.

2.4) Model characterization

Geometric surface area of the modelled materials was computed using Monte Carlo (MC) on RASPA 2.0 software (48), where a probe atom (radius σ = 2.958 Å) was "rolled" over the AC model surface, and the S_{BET} was considered as the summation of all non-overlapping probe spheres after 10^4 steps. Additionally, void fraction volumes were also computed using MC. Helium probes were inserted in the AC model box using Widom particle insertions, and the void fraction was determined to be the empty space divided by the total volume.

Molecular structures were visualized with PyMol (49). Pore studies were performed with the aid of MOLE 2.0 software (50), considering only pores with diameters less than 2 nm (micropores). A 30 Å surface probe was used to find cavities.

2.5) Monte Carlo adsorption essays

Within the scope of the present work, sulfamethoxazole (SMX) and carbamazepine (CBZ), two pharmaceutical compounds frequently found in the environment (51–53), are proposed as target active agents for adsorption. A multi conformational analysis was first employed where the molecules were brought up to 1500 K and left to relax, in order to adopt possible new conformations. Molecule optimizations of the low energy conformations were then carried by DFT at B3LYP/6-31G* level, with RESP charges determination, at pH of 7.

Monte Carlo adsorption essays were carried out in the GCMC ensemble using RASPA 2.0 software. Partial pressure values were converted to fugacity using the Peng-Robinson equation

of state (54). Critical temperature (TC), critical pressure (PC) and acentric factor (ω) values were extracted from available literature for water and ions. SMX and CBZ critical properties were estimated using Joback method (55), and acentric factors were predicted using Positional Distributive Contribution method (56). The calculated values used in the present work are available in Table 1. GCMC essays were performed for $3x10^3$ to $6x10^3$ steps (or until equilibrium), at 300 K and 1 atm. Water was used as solvent in all essays. Partial pressures of the components in the simulation were tuned to reflect the desired concentration of the pharmaceutical molecules in the mixture.

Simulated concentrations of pharmaceuticals in water were 1, 100 and 1000 ppb, as to reflect the values commonly found in literature regarding their concentrations in the environment. Two modes of adsorption were studied: single component and competitive adsorption. In competitive adsorption, the considered pharmaceuticals were in an equimolar mixture. In the GCMC ensemble, four types of moves were employed, with equal probability: translation, rotation, reinsertion and identity change.

3. RESULTS AND DISCUSSION

3.1) Experimental data

AC production overall yield was 3.5%, resulting in an extremely low-density material (apparent density of 0.09 g cm^{-3} (32)). Six characterization techniques were explored. The most relevant results are as follows:

The PZC for the AC sample was determined to be in the pH range between 5 and 6. This means that for pH values inferior to the PZC, AC functional groups in the computational model should be protonated, and vice-versa. Since, for this work, a pH of 7 was chosen for the adsorption medium (since it is the commonly found value in WWTPs), all functional groups are negatively charged.

Ultimate analysis allows for the determination of the elemental composition of the sample. For the purpose of modelling the AC sample, values are shown in chemical amount (*n*, %). The

produced AC sample composition in dry and ash free basis is mostly comprised of carbon (73.2±0.2%), with a high content of oxygen (24.3±0.4%). The remaining fraction consists of hydrogen (1.9±0.6%), nitrogen (0.62±0.04%) and sulphur (0.03±0.01%) atoms (Figure 1). For simplification purposes, and considering the relatively low contributions of both elements (below 1%), neither nitrogen and sulphur atoms were considered in the proposed model.

S_{BET} analysis show that the produced AC sample has a specific surface area of 1586 m^2 g^{-1}. This value places the produced AC in the present work on pair with available commercial products. By comparison, the commercially available PULSORB RD 90 has a S_{BET} of 1100 m^2 g^{-1} (57) and the YP50F has a S_{BET} of 1600 m^2 g^{-1} (58). Furthermore, the average pore diameter in the AC sample was determined to be 2.93 nm, with approximately 32% of the total pore volume (0.839 cm^3 g^{-1}) resulting from micropores (0.268 cm^3 g^{-1}).

Functional group content was determined by XPS. This technique allows for the surface characterization with a depth of analysis up to 10 nm. The gathered data shows that the majority of the carbon layers are composed of sp^2 carbon (54.4%) with some functionalization level of carbon atoms as -CH (8.5%), ethers (15.9%), carboxylic (2.9%) and carbonyl (8.4%).

SEM and TEM images are displayed in Figure 2. SEM images allow the visualization of a porous network and TEM images show that AC carbon walls are, in fact, amorphous and rugged, possibly due to the presence of meso- and micropores.

In an effort to more accurately simulate AC samples, the complete characterization of the experimental material provided a starting point for the development of the proposed computational model, albeit a certain level of approximation was required.

3.2) VPC model development

The construction of the proposed VPC model was divided into 2 stages: firstly, the residue library assembly and secondly the VPC clustering process.

As proposed by Rosalin E. Franklin in 1951 (59), and later implemented in the first VPC models by Segarra and Glandt in 1994 (60), microcrystallites of carbon layers were employed as the building blocks of the AC model. This molecular organization of the AC samples seems to be in agreement with TEM imaging (Figure 2). The residues (or platelets) were composed of 1-4 parallel graphite-like layers (3.14 Å gap), each with approximately 20 Å length and width.

Residues were then decorated with different functional groups (FG) namely -CH terminations, ethers (in both 2- and 3-ring conformations), carboxyls and carbonyls (See F2 in Supporting Information). The quantity of each functional group added was in accordance to XPS data.

Smaller residues were built for atom partial charge determination, and the presence of a single functional group was studied at a time. Such residues were optimized by DFT and the charges determined by RESP. The employed charges are displayed in the Supporting Information T1. As previously stated, carboxyl groups (COO^-) were left deprotonated and with a negative charge (-1 e^-), as reported in PZC determination essays. A random Gaussian distribution was employed in the input experimental values to generate small variances in the different residues of each library, in an effort to better reproduce the real heterogeneity of the carbon materials. A residue library was composed of at least 100 different residue microcrystallites similar to Figure 3. A more detailed description of the software developed can be found in the Supporting Information.

A free working version of the developed tool (CarbGen) can be found online, at carbgen.web.ua.pt, allowing for an easy assembly of carbon residue libraries with varying sizes and different types and quantities of FGs.

After assembly of an adequate library of residues, it was possible to continue to the VPC clustering process by molecular dynamics. A random number of residues was arbitrarily placed

inside a cubic simulation box and the carbon atom count limit was placed at 3 000 atoms per simulation, in order to keep the complexity of the system and the clustering time as low as possible without compromising the relevance of the obtained results. The maximum number of insertion attempts of new residues was tuned to ensure that all available space was occupied, and the void fraction of the box was solely modulated by the size of the residues. The system was then left to minimize through molecular dynamics simulation in vacuum. Simulations were performed in the NVT ensemble (no pressure coupling); translation/rotation around the system center of mass were removed in all simulations. The proposed residue clustering process was composed of 3 distinct stages:

Minimization: The system was initially relaxed. Minimization criteria were: $F_{max} < 10$ kJ mol^{-1} nm^{-1}, 100 000 steps or ΔF lower than machine tolerance;

Heating: The system was brought up to 300 K, allowing the molecules to adopt higher energy conformations and cluster together during 1 to 2 ns.

Stabilization: The carbon models were left to stabilize at 300 K for 1 to 2 ns, for data gathering (every 1000 steps) and pore development. The LINCS algorithm was applied to convert all bonds and angles that involve hydrogen atoms to bond constrains.

A visual depiction of the clustered AC model is illustrated in Figure 4.

3.3) Model validation

Although the experimental sample of AC had an S_{BET} of 1586 m^2 g^{-1}, the computational model showed an S_{BET} of 2043 ± 200 m^2 g^{-1}. This difference can be explained by the existence of residual and non-simulated impurities, such as carbonates, in the real sample which block access to pores in S_{BET} experimental essays, or the existence of enclosed cavities in the AC sample, inaccessible to the probe molecule in S_{BET} determination, but accounted for in the computational MC method. Nonetheless, given the fact that surface area in the proposed model had no parametrization guidelines, resulting solely on the natural minimization of the modeled residues, it is considered that the deviation from the experimental value does not critically hinder the present work.

The agreement of the current model with experimental data was evaluated. As visible in Figure 1, elemental composition of both the experimental material and the VPC model are in good conformity. Furthermore, functional content was also successfully parametrized in accord with experimental data, as shown in Figure 5. The observed difference in -CH group content between the experimental sample and the VPC may hint at a lack of disorder in the computational model, where an increase in microporous structure would consequentially increase –CH content. Also, minor defects (pores) in the outmost layers of each microcrystallite can help increase –CH content without contributing to an increase on the microporosity.

The formation and development of micropores in the proposed model was also studied. Pore structure has been appointed as an important factor in different applications, such as adsorption. Therefore, the model here proposed should be able to develop an organized, complex and viable micropore structure. Such challenge, although not trivial, is considered to be accomplished in the developed AC models (Figure 6).

3.4) Monte Carlo adsorption essays

With the developed CarbGen tool it is possible to easily create VPC models with different surface chemistry characteristics. Distinct residue libraries were built, with different levels of oxygen, as shown in Figure 7.

With the increase of oxygen levels, the resulting microcrystallites progressively diverge from the initial planar form, and take a rougher structural shape, due to the sp^3 hybridization of the majority of the functional groups added during functionalization, therefore promoting loss of aromaticity of the carbon backbone and planarity of the microcrystallites. This, in turn, results in the increase of the carbon surface area, as shown in Figure 8.

GCMC ensemble simulations were then employed to perform adsorption essays of CBZ and SMX onto the produced models (with the designations of minOx, fullOx, maxOx for the models who represent the minimum, experimental and maximum value for oxygen, respectively). Three replicas were performed for each carbon model, additionally, in order to evaluate both the inter- and intra-model variations. Maximum adsorption capacities were calculated for each library

model and are shown in Figure 9. For each AC model, two modes of adsorption were considered: single component (SC – only 1 pharmaceutical at a time) and competitive adsorption (C – both SMX and CBZ were added to the simulation simultaneously). This allows for the study of possible competitive or cooperative adsorption mechanisms of these pharmaceuticals. Overall, results suggest that pharmaceutical adsorption increases with increasing oxygen content (≈ 20x and 6x increase for CBZ and SMX, respectively, in SC mode, from minOx to maxOx models). Competitive adsorption showed lower adsorption values for each pharmaceutical, as expected, although not significant or within the errors of the SC mode essay. This suggests the existence of some degree of cooperative adsorption or double layer effects, where a second pharmaceutical molecule is adsorbed onto the surface of a first already adsorbed to the carbon surface. Finally, it is possible to observe a clear distinction between the adsorption of the two pharmaceuticals.

For the maxOx model, CBZ had an adsorption capacity *ca.* 2x superior to SMX. Since the simulations were carried at neutral pH of 7, both SMX (pKa_1 = 1.8; pKa_2 = 5.7 (61)) and the AC are negatively charged and repulse each other. This does not apply to CBZ (pKa = 13.9 (61)), which is neutral at pH 7. As previously discussed, an increase in oxygen content of the AC models resulted in an equal increase in the surface area which, consequently, has positive repercussions in adsorption capacities. However, it is possible to infer that the increased SMX adsorption by carbons with high oxygen content (and, therefore, charge) is caused by the increase in the AC surface area, while an increase in oxygen content has an additional positive effect in CBZ adsorption. Although being a neutral species at pH 7, CBZ can have induced dipole moments that interact with negatively charged functional groups of the AC. This result hints at the importance of functional groups and electrostatic interactions as modulators of adsorption and/or specificity in AC adsorbents.

Further work is envisioned with the experimental determination of the adsorption isotherms, both in single component and competitive modes, allowing comparison of the maximum adsorption capacities determined experimentally to those calculated with the developed model,

which would complement the validation of the physico-chemical characterization of the model, described in this study. Also, manipulation of the oxygen content of real samples through adequate functionalization will provide the necessary mechanisms to fully assess the influence of oxygen content on the adsorption capabilities of organic molecules by activated carbons.

4. CONCLUSION

In a first instance, AC production from paper mill PS was explored, resulting in an interesting material with S_{BET} values competitive with existing commercial solutions.

Some VPC models of AC have been previously presented. However, literature data from different sources was commonly utilized as input for the parametrization of the referred models and not much emphasis was given to surface chemistry as a modulator of the final characteristics of the model. Therefore, in the present work, AC model development had an experimental basis on top of which more quantitatively accurate VPC models were built. It is shown that elemental composition, functional group content, surface area and pore structure are in good accordance to the gathered experimental data. This constitutes a validated computational model of the AC sample. Furthermore, an online tool has been developed and made freely available, allowing for easy modeling of ACs with specific surface chemistry characteristics.

Such a model constitutes a workhorse for easily running simulations with the aim of gathering evidence about the underlying mechanisms of adsorption of molecules of interest from aqueous solutions in a more reproducible way. It was possible to observe the increase in surface area with the increase of oxygen content. This resulted in the increase of both SMX and CBZ adsorption capacities. Moreover, the additional charged FGs had a further positive effect in the adsorption capacity of CBZ, reinforcing the idea that AC adsorption optimization varies in accordance to the target molecules.

The modelling approach described in this work is broad and easily adjustable, paving the way for adaptation in future developments. Modifications to the current algorithm will quickly and

reliably allow modelling of different materials, such as graphene oxides, clays, ceramics and silicates, among others.

Acknowledgments

This work was funded by FEDER through COMPETE 2020 and by national funds through FCT by the research project PTDC/AAG-TEC/1762/2014. Thanks are also due for the financial support to CICECO-Aveiro Institute of Materials, POCI-01-0145-FEDER-007679 (FCT Ref. UID /CTM /50011/2013) and to CESAM (UID/AMB/50017/2013) financed by FCT/MEC through national funds, and the co-funding by the FEDER, within the PT2020 Partnership Agreement and Compete 2020. Vânia Calisto and Sérgio Santos also thank FCT for a postdoctoral grant (SFRH/BPD/78645/2011) and support by the FCT Investigator Program (IF/00973/2014), respectively.

REFERENCES

1. Escher BI, Baumgartner R, Lienert J, Fenner K. Predicting the ecotoxicological effects of transformation products. Handb Environ Chem Vol 2 React Process. 2009;2 P:205–44.
2. Boxall ABA, Sinclair CJ, Fenner K, Kolpin D, Maund SJ. Peer reviewed: When synthetic chemicals degrade in the environment. Environ Sci Technol. 2004;38(19):368A–375A.
3. Jelić A, Petrović M, Barceló D. Pharmaceuticals in Drinking Water. The Handbook of Environmental Chemistry. Springer Berlin Heidelberg; 2012. p. 1–24.
4. Escher BI, Fenner K. Recent advances in environmental risk assessment of transformation products. Vol. 45, Environmental Science and Technology. 2011. p. 3835–47.
5. Leal JE, Thompson AN, Brzezinski W a. Pharmaceuticals in drinking water: local analysis of the problem and finding a solution through awareness. J Am Pharm Assoc (2003). 2010;50(5):600–3.
6. Jones OA, Lester JN, Voulvoulis N. Pharmaceuticals: A threat to drinking water? Vol. 23, Trends in Biotechnology. 2005. p. 163–7.
7. Boxall AB a. The environmental side effects of medication. EMBO Rep. 2004;5(12):1110–6.
8. European Commision. COM(2011) 876: amending Directives 2000/60/EC and 2008/105/EC as regards priority substances in the field of water policy. Brussels; 2011.

9. Zwiener C, Frimmel FH. Oxidative treatment of pharmaceuticals in water. Water Res. 2000;34(6):1881–5.
10. Mirzaei A, Chen Z, Haghighat F, Yerushalmi L. Removal of pharmaceuticals from water by homo/heterogonous Fenton-type processes – A review. Chemosphere. 2017;174:665–88.
11. Kim I, Yamashita N, Tanaka H. Performance of UV and UV/H_2O_2 processes for the removal of pharmaceuticals detected in secondary effluent of a sewage treatment plant in Japan. J Hazard Mater. 2009;166(2–3):1134–40.
12. Ziylan A, Ince NH. The occurrence and fate of anti-inflammatory and analgesic pharmaceuticals in sewage and fresh water: Treatability by conventional and non-conventional processes. Vol. 187, Journal of Hazardous Materials. 2011. p. 24
13. Rodriguez-Narvaez OM, Peralta-Hernandez JM, Goonetilleke A, Bandala ER. Treatment technologies for emerging contaminants in water: A review. Chem Eng J. 2017;323:361–80.
14. Adams C, Wang Y, Loftin K, Meyer M. Removal of Antibiotics from Surface and Distilled Water in Conventional Water Treatment Processes. J Environ Eng. 2002;128(3):253–60.
15. Thue PS, Adebayo MA, Lima EC, Sieliechi JM, Machado FM, Dotto GL, et al. Preparation, characterization and application of microwave-assisted activated carbons from wood chips for removal of phenol from aqueous solution. J Mol Liq. 2016;223:1067–80.
16. Ould-Idriss A, Stitou M, Cuerda-Correa EM, Fernández-González C, Macías-García A, Alexandre-Franco MF, et al. Preparation of activated carbons from olive-tree wood revisited. I. Chemical activation with H3PO4. Fuel Process Technol. 2011;92(2):261–5.
17. Rodriguez-Narvaez OM, Peralta-Hernandez JM, Goonetilleke A, Bandala ER. Treatment technologies for emerging contaminants in water: A review. Vol. 323, Chemical Engineering Journal. 2017. p. 361–80.
18. Cossarutto L, Zimny T, Kaczmarczyk J, Siemieniewska T, Bimer J, Weber J V. Transport and sorption of water vapour in activated carbons. Carbon N Y. 2001;39(15):2339–46.
19. Ngernyen Y, Tangsathitkulchai C, Tangsathitkulchai M. Porous properties of activated carbon produced from Eucalyptus and Wattle wood by carbon dioxide activation. Korean J Chem Eng. 2006;23(6):1046–54.
20. Giraldo L, Moreno-Piraján JC. Pb^{2+} adsorption from aqueous solutions on activated carbons obtained from lignocellulosic residues. Brazilian J Chem Eng. 2008;25(1):143–51.
21. González-García P. Activated carbon from lignocellulosics precursors: A review of the synthesis methods, characterization techniques and applications. Vol. 82, Renewable and Sustainable Energy Reviews. Pergamon; 2018. p. 1393–414.
22. Danish M, Ahmad T. A review on utilization of wood biomass as a sustainable precursor for activated carbon production and application. Vol. 87, Renewable and Sustainable Energy Reviews. Pergamon; 2018. p. 1–21.

23. Wakizaka H, Miyake H, Kawahara Y. Utilization of beer lees waste for the production of activated carbons: The influence of protein fractions on the activation reaction and surface properties. Sustain Mater Technol. 2016;8:1–4.
24. Brito MJP, Veloso CM, Bonomo RCF, Fontan R da CI, Santos LS, Monteiro KA. Activated carbons preparation from yellow mombin fruit stones for lipase immobilization. Fuel Process Technol. 2016;
25. Calisto V, Ferreira CIA, Oliveira JABP, Otero M, Esteves VI. Adsorptive removal of pharmaceuticals from water by commercial and waste-based carbons. J Environ Manage. 2015;152:83–90.
26. Jaria G, Calisto V, Gil MV, Otero M, Esteves VI. Removal of fluoxetine from water by adsorbent materials produced from paper mill sludge. J Colloid Interface Sci. 2015;448:32–40.
27. Jaria G, Silva CP, Ferreira CIA, Otero M, Calisto V. Sludge from paper mill effluent treatment as raw material to produce carbon adsorbents: An alternative waste management strategy. J Environ Manage. 2017;188:203–11.
28. Calisto V, Ferreira CIA, Santos SM, Gil MV, Otero M, Esteves VI. Production of adsorbents by pyrolysis of paper mill sludge and application on the removal of citalopram from water. Bioresour Technol. 2014;166:335–44.
29. Ferreira CIA, Calisto V, Otero M, Nadais H, Esteves VI. Comparative adsorption evaluation of biochars from paper mill sludge with commercial activated carbon for the removal of fish anaesthetics from water in Recirculating Aquaculture Systems. Aquac Eng. 2016;74:76–83.
30. Coimbra RN, Calisto V, Ferreira CIA, Esteves VI, Otero M. Removal of pharmaceuticals from municipal wastewater by adsorption onto pyrolyzed pulp mill sludge. Arabian Journal of Chemistry. 2015;
31. Ferreira CIA, Calisto V, Otero M, Nadais H, Esteves VI. Removal of tricaine methanesulfonate from aquaculture wastewater by adsorption onto pyrolysed paper mill sludge. Chemosphere. 2017;168:139–46.
32. Jaria G, Silva CP, Oliveira JABP, Santos SM, Gil MV, Otero M, et al. Production of highly efficient activated carbons from industrial wastes for the removal of pharmaceuticals from water—A full factorial design. J Hazard Mater. 2018;
33. Boshoff S, Gottumukkala LD, van Rensburg E, Görgens J. Paper sludge (PS) to bioethanol: Evaluation of virgin and recycle mill sludge for low enzyme, high-solids fermentation. Bioresour Technol. 2016;203:103–11.
34. Areeprasert C, Scala F, Coppola A, Urciuolo M, Chirone R, Chanyavanich P, et al. Fluidized bed co-combustion of hydrothermally treated paper sludge with two coals of different rank. Fuel Process Technol. 2016;144:230–8.

35. Fang S, Yu Z, Lin Y, Hu S, Liao Y, Ma X. Thermogravimetric analysis of the co-pyrolysis of paper sludge and municipal solid waste. Energy Convers Manag. 2015;101:626–31.
36. Xu C, Lancaster J. Conversion of secondary pulp/paper sludge powder to liquid oil products for energy recovery by direct liquefaction in hot-compressed water. Water Res. 2008;42(6–7):1571–82.
37. Phan NH, Rio S, Faur C, Le Coq L, Le Cloirec P, Nguyen TH. Production of fibrous activated carbons from natural cellulose (jute, coconut) fibers for water treatment applications. Carbon N Y. 2006;44(12):2569–77.
38. Liu JC, Monson PA. Monte Carlo simulation study of water adsorption in activated carbon. Ind Eng Chem Res. 2006;45(16):5649–56.
39. Di Biase E, Sarkisov L. Systematic development of predictive molecular models of high surface area activated carbons for adsorption applications. Carbon N Y. 2013;64:262–80.
40. Gonciaruk A, Siperstein FR. In silico designed microporous carbons. Carbon N Y. 2015;88:185–95.
41. Bahamon D, Carro L, Guri S, Vega LF. Computational study of ibuprofen removal from water by adsorption in realistic activated carbons. J Colloid Interface Sci. 2017;498:323–34.
42. Biggs MJ, Buts A. Virtual porous carbons: What they are and what they can be used for. Mol Simul. 2006;32(7):579–93.
43. Wang J, Wolf RM, Caldwell JW, Kollman PA, Case DA. Development and testing of a general Amber force field. J Comput Chem. 2004;25(9):1157–74.
44. Frisch MJ, Trucks GW, Schlegel HB, Scuseria GE, Robb MA, Cheeseman JR, et al. Gaussian 09, Revision B.01. Gaussian 09, Revision B.01, Gaussian, Inc., Wallingford CT. 2009.
45. Wang J, Wang W, Kollman PA, Case DA. Automatic atom type and bond type perception in molecular mechanical calculations. J Mol Graph Model. 2006;25(2):247–60.
46. Abraham MJ, Murtola T, Schulz R, Páll S, Smith JC, Hess B, et al. Gromacs: High performance molecular simulations through multi-level parallelism from laptops to supercomputers. SoftwareX. 2015;1–2:19–25.
47. Jorgensen WL, Chandrasekhar J, Madura JD, Impey RW, Klein ML. Comparison of simple potential functions for simulating liquid water. J Chem Phys. 1983;79(2):926–35.
48. Dubbeldam D, Calero S, Ellis DE, Snurr RQ. RASPA: Molecular simulation software for adsorption and diffusion in flexible nanoporous materials. Mol Simul. 2016;42(2):81–101.
49. Schrödinger, LLC. The {PyMOL} Molecular Graphics System, Version~1.8. 2015.
50. Sehnal D, Vařeková RS, Berka K, Pravda L, Navrátilová V, Banáš P, et al. MOLE 2.0: Advanced approach for analysis of biomacromolecular channels. J Cheminform. 2013;5(8):39.

51. Johnson AC, Jürgens MD, Nakada N, Hanamoto S, Singer AC, Tanaka H. Linking changes in antibiotic effluent concentrations to flow, removal and consumption in four different UK sewage treatment plants over four years. Environ Pollut. 2017;220:919–26.
52. Johnson AC, Keller V, Dumont E, Sumpter JP. Assessing the concentrations and risks of toxicity from the antibiotics ciprofloxacin, sulfamethoxazole, trimethoprim and erythromycin in European rivers. Sci Total Environ. 2015;511:747–55.
53. Andreozzi R, Marotta R, Pinto G, Pollio A. Carbamazepine in water: Persistence in the environment, ozonation treatment and preliminary assessment on algal toxicity. Water Res. 2002;36(11):2869–77.
54. Peng DY, Robinson DB. A New Two-Constant Equation of State. Ind Eng Chem Fundam. 1976;15(1):59–64.
55. JOBACK KG, REID RC. Estimation of pure-component properties from group-contributions. Chem Eng Commun. 1987;57(1–6):233–43.
56. Wang Q, Jia Q, Ma P. Prediction of the acentric factor of organic compounds with the positional distributive contribution method. J Chem Eng Data. 2012;57(1):169–89.
57. Ivancev-Tumbas I, Hobby R. Removal of organic xenobiotics by combined out/in ultrafiltration and powdered activated carbon adsorption. Desalination. 2010;255(1–3):124–8.
58. Yang I, Kwon D, Kim M-S, Jung JC. A comparative study of activated carbon aerogel and commercial activated carbons as electrode materials for organic electric double-layer capacitors. Carbon N Y. 2018;132:503–11.
59. Franklin RE. Crystallite Growth in Graphitizing and Non-Graphitizing Carbons. Proc R Soc A Math Phys Eng Sci. 1951;209(1097):196–218.
60. Segarra EI, Glandt ED. Model microporous carbons: microstructure, surface polarity and gas adsorption. Chem Eng Sci. 1994;49(17):2953–65.
61. Oliveira G, Calisto V, Santos SM, Otero M, Esteves VI. Paper pulp-based adsorbents for the removal of pharmaceuticals from wastewater: A novel approach towards diversification. Sci Total Environ. 2018;631–632:1018–28.

Table 1. Critical properties and acentric factors calculated for the pharmaceutical molecules studied

	T_C (K)	P_C (kPa)	ω
SMX	1006.40	5175.72	0.2389
CBZ	915.59	3325.84	0.1456

Figure captions

Figure 1. Elemental composition comparison between experimental AC sample and the proposed computational model.

Figure 2. SEM and TEM images of the produced AC sample. (a) – SEM, 300x; (b) – SEM, 3 000x; (c) – SEM, 10 000x; (d) – SEM, 50 000x; (e) – TEM, 5 000x; (f) – TEM, 50 000x; (g) – TEM, 100 000x; (h) – TEM, 200 000x.

Figure 3. Example of an assembled residue. Over 100 different residues were assembled in a library for random incorporation in AC models.

Figure 4. Instance of the proposed AC model after clustering process.

Figure 5. Functional content comparison between the proposed AC model and experimental data.

Figure 6. Elucidated micropore structure of the proposed model. Top – Model and pore structure. Bottom – Pore structure

Figure 7. Different produced VPC models, with varying levels of oxygen content: **Top**- minOx, 1.5% O; **Middle** – fullOx, 18.9% O; **Bottom** – maxOx, 24.3% O.

Figure 8. Surface area evolution with oxygen content.

Figure 9. GCMC adsorption results for different AC models, regarding CBZ and SMX in single component.

Highlights

- Activated carbon (AC) was produced from paper mill sludge, with S_{BET} of 1586 m^2 g^{-1}
- A full functional and elemental characterization of the obtained material is given
- Characterization data was used to parametrize a quantitative AC computational model
- An online tool for the creation of AC models is made available
- Monte Carlo simulations were used to study drug adsorption onto the developed model

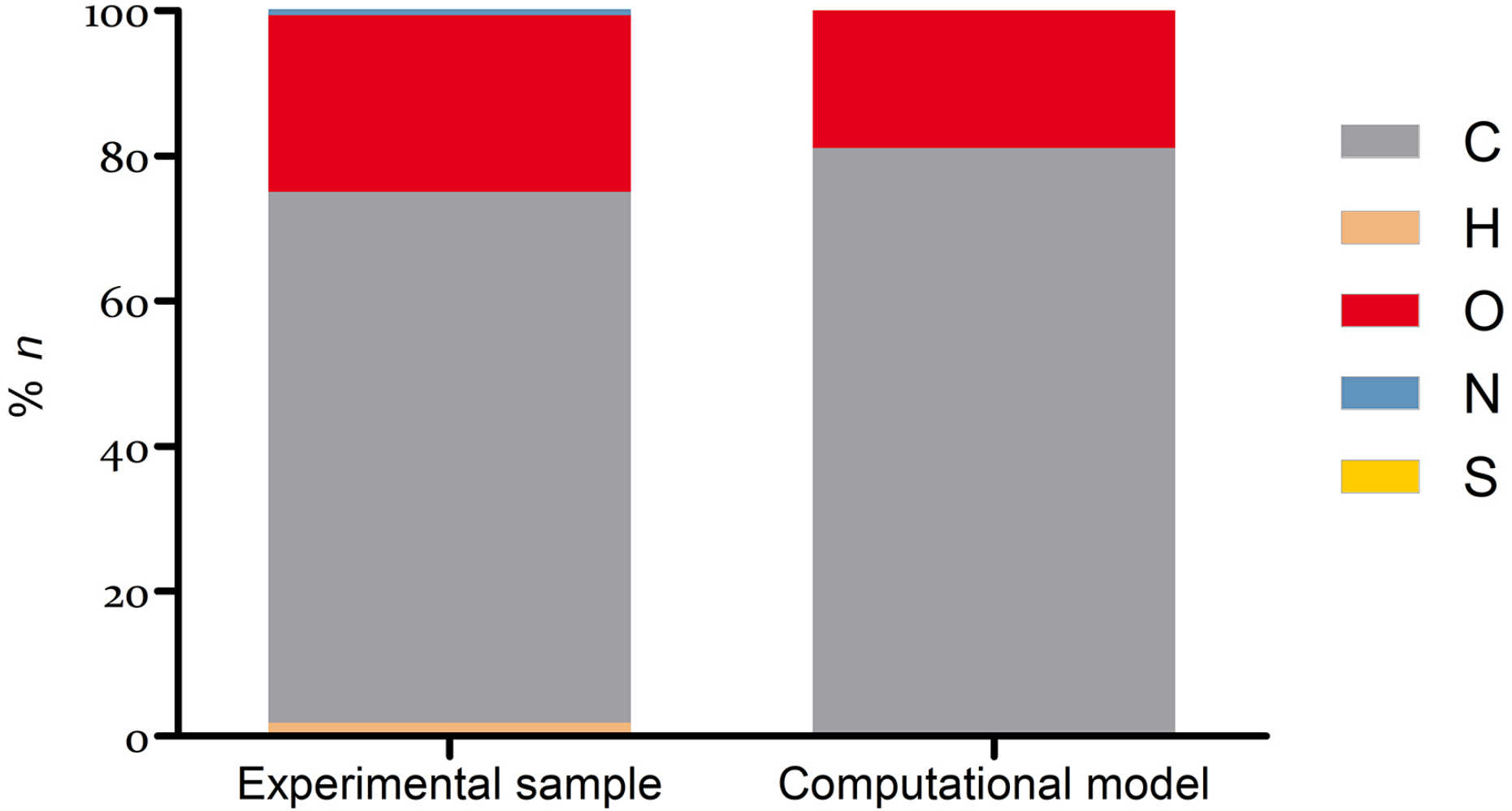
100
80
60
40
20
0
% n
Experimental sample
Computational model
C
H
O
N
S

Figure 1

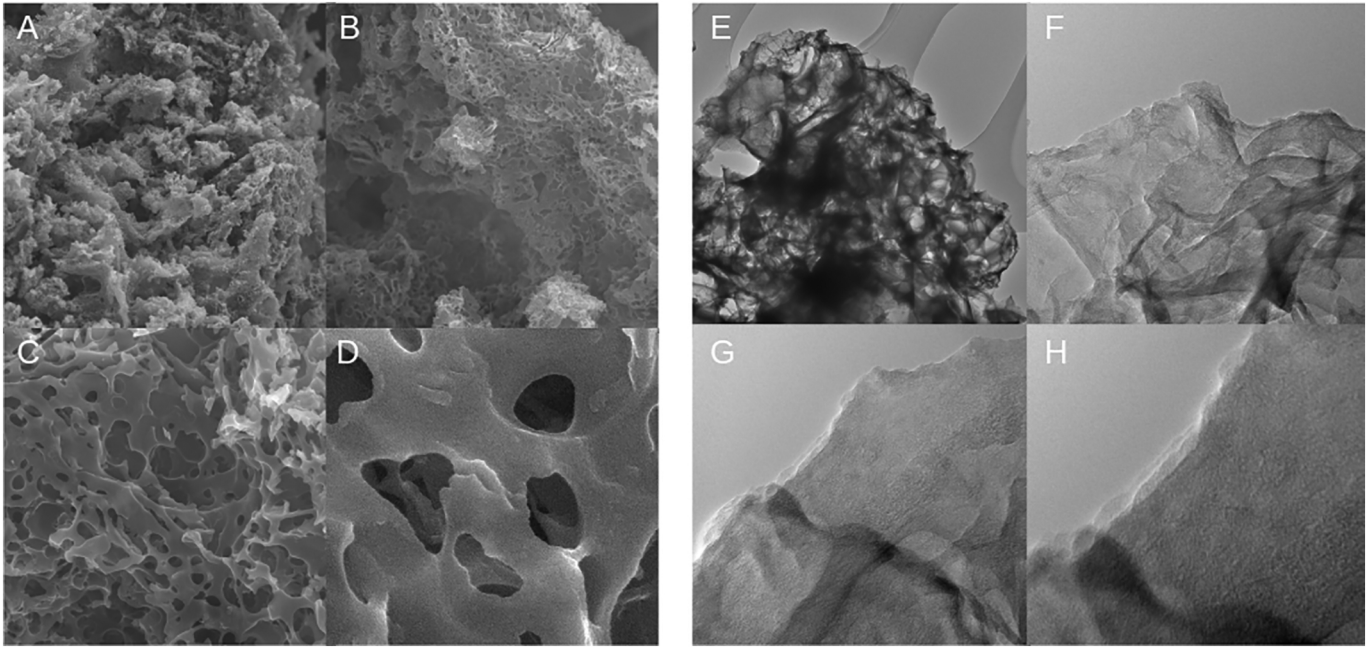

Figure 2

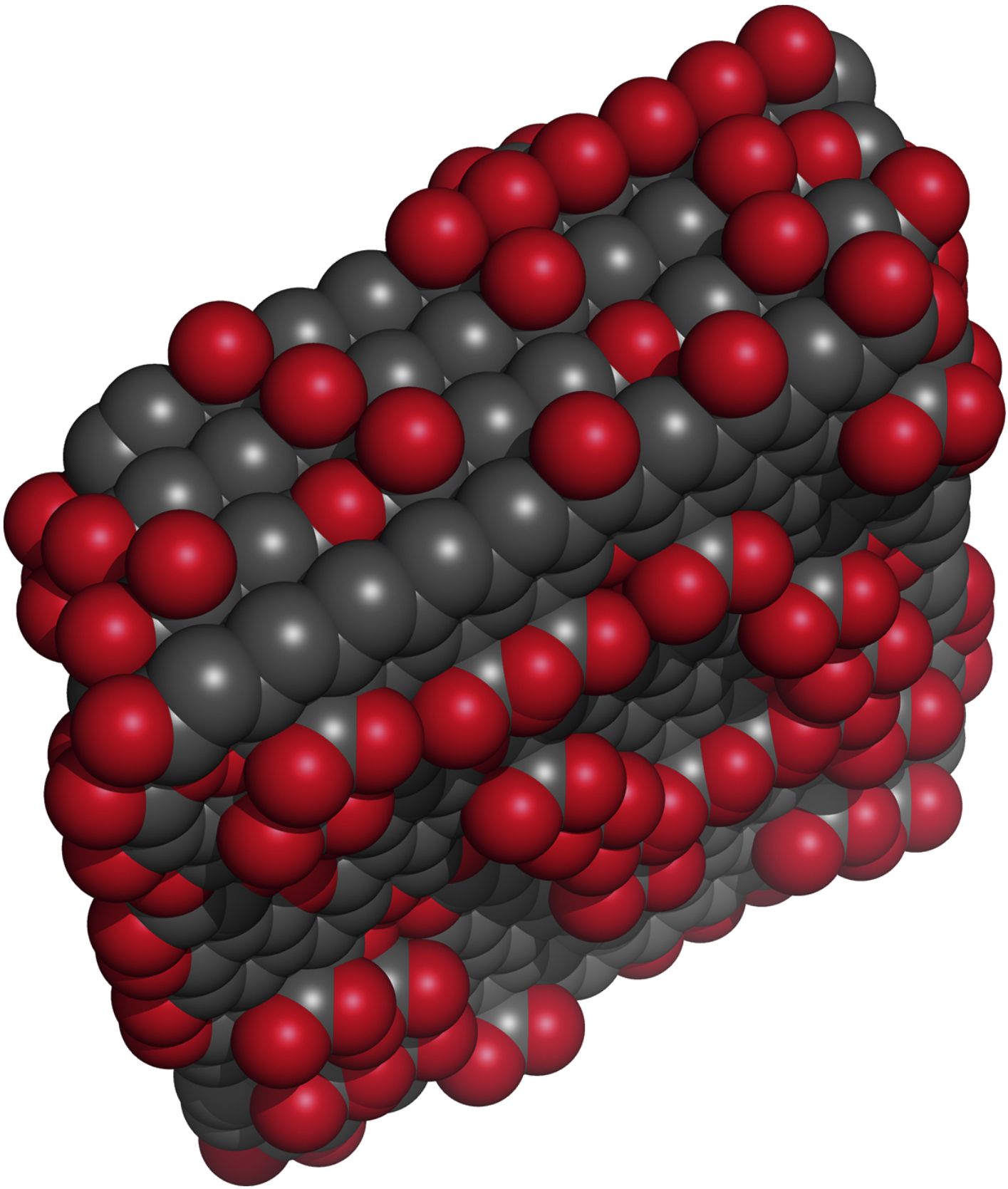

Figure 3

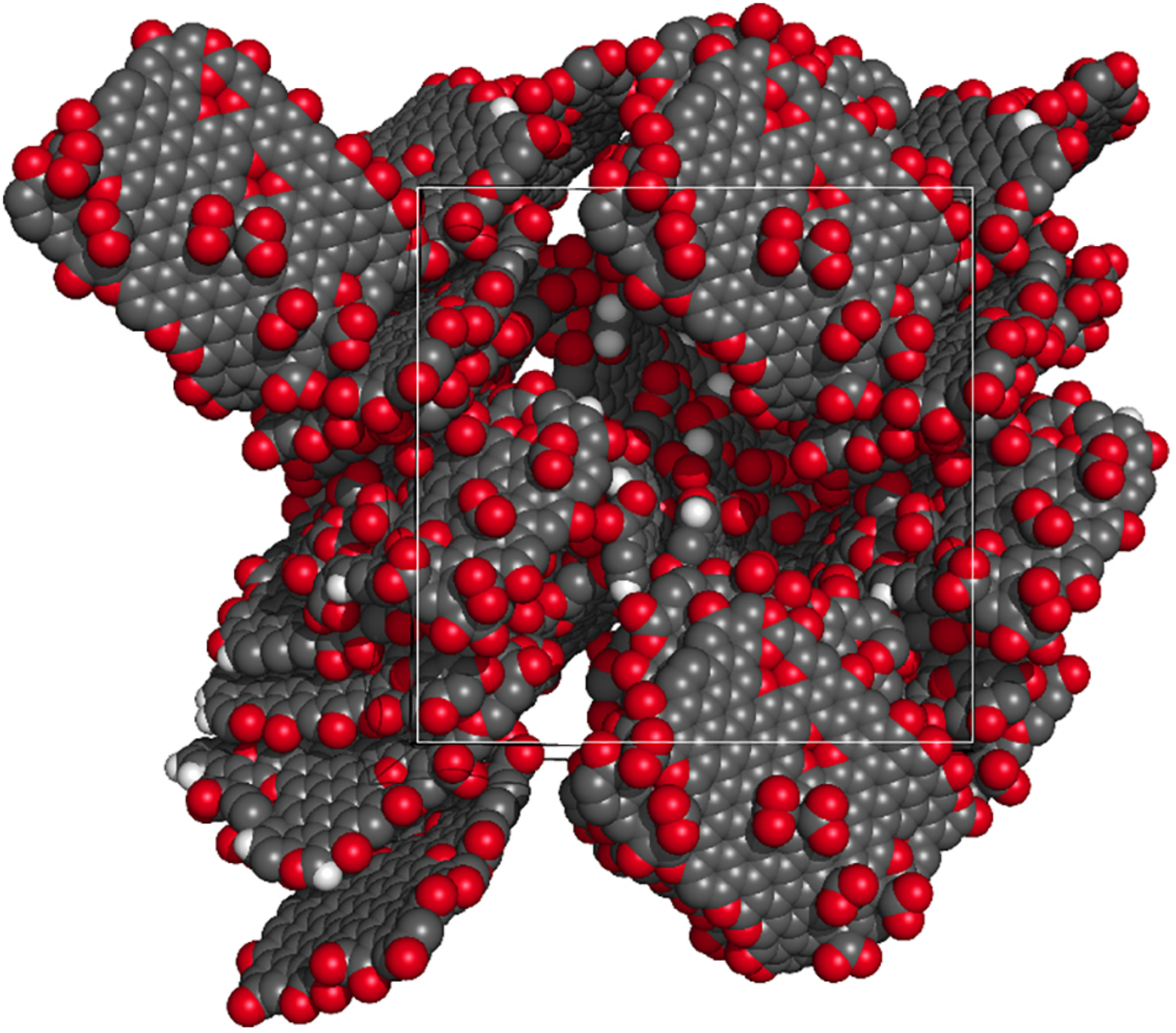

Figure 4

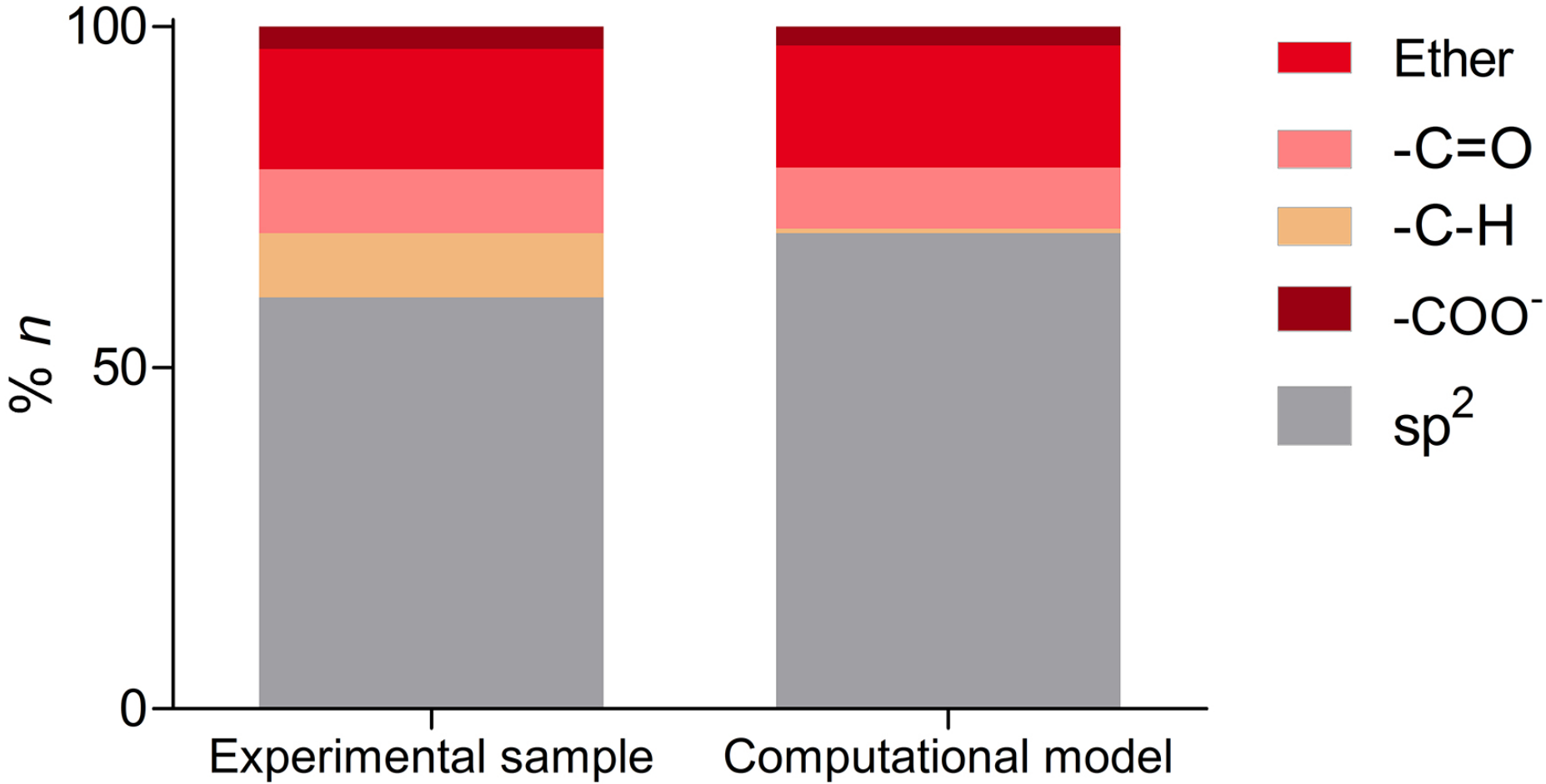
100
50
0
% n
Experimental sample
Computational model
Ether
-C=O
-C-H
-COO-
sp2

Figure 5

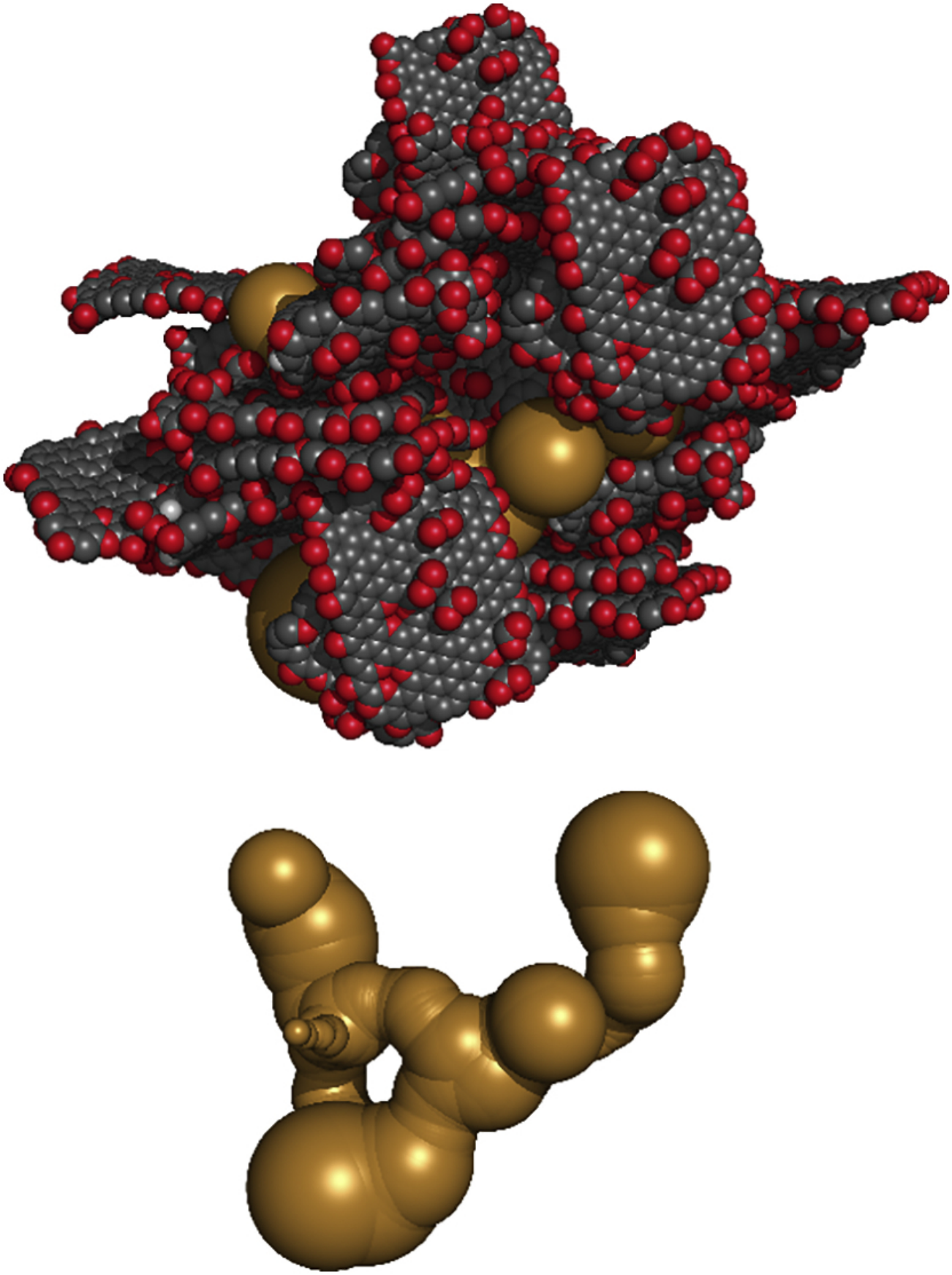

Figure 6

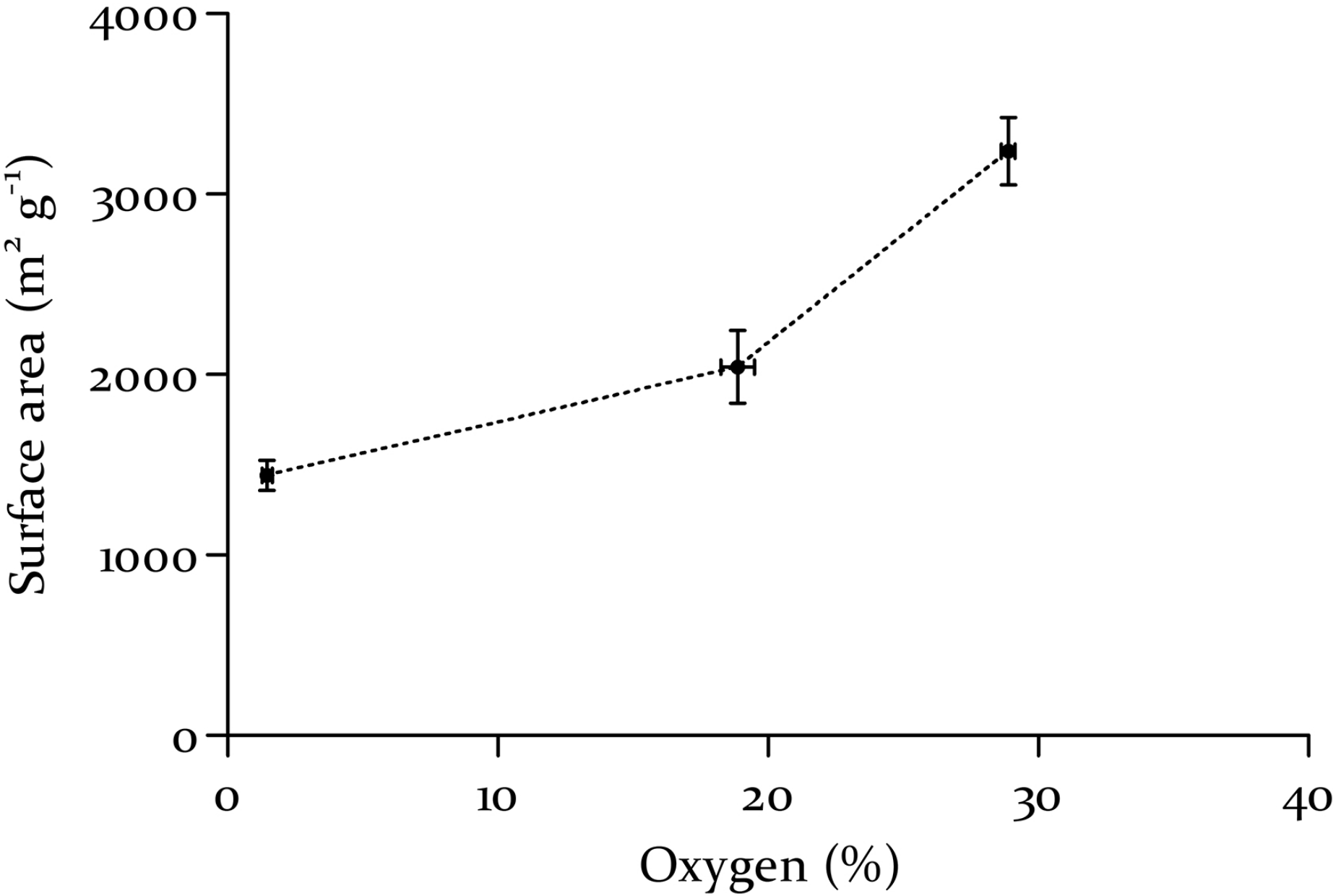

Figure 7

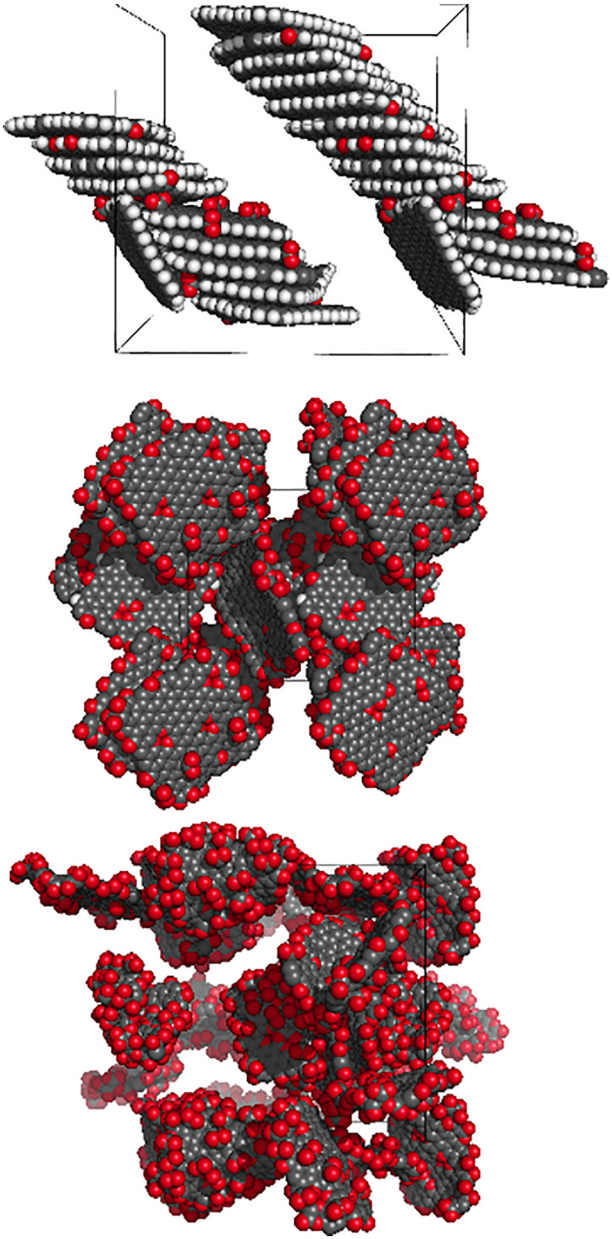

Figure 8

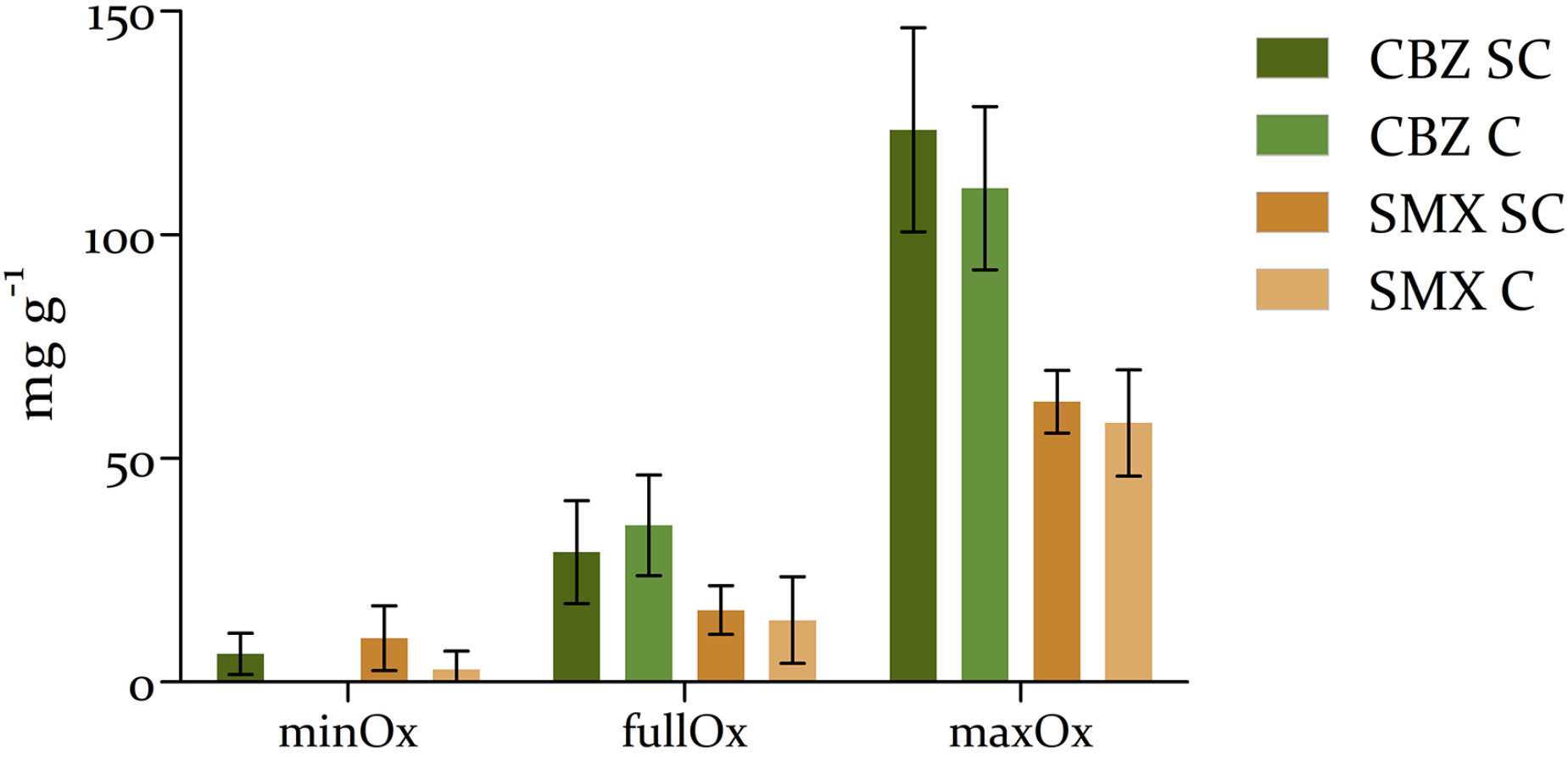

Figure 9